Supplement of Solid Earth, 17, 465–484, 2026
https://doi.org/10.5194/se-17-465-2026-supplement

Solid Earth Open Access EGU

Supplement of

Constraining the wavefield of volcano-seismic events on Mt. Etna, Italy through a rotational sensor and seismic array observations

Nele Inken Käte Vesely et al.

Correspondence to: Nele Inken Käte Vesely (vesely1@uni-potsdam.de)

frequency [1/s]	velocity [m/s]	source depth [m]	uncertainty [m]
0.6	500	510	460.98
0.6	500	600	500.0
0.6	1000	510	651.92
0.6	1000	600	707.11
1.4	500	510	301.78
1.4	500	600	327.33
1.4	1000	510	426.78
1.4	1000	600	462.91

Table S1: Combinations of frequency, velocity and source depth used for the INGV-OE LP location uncertainty calculation.

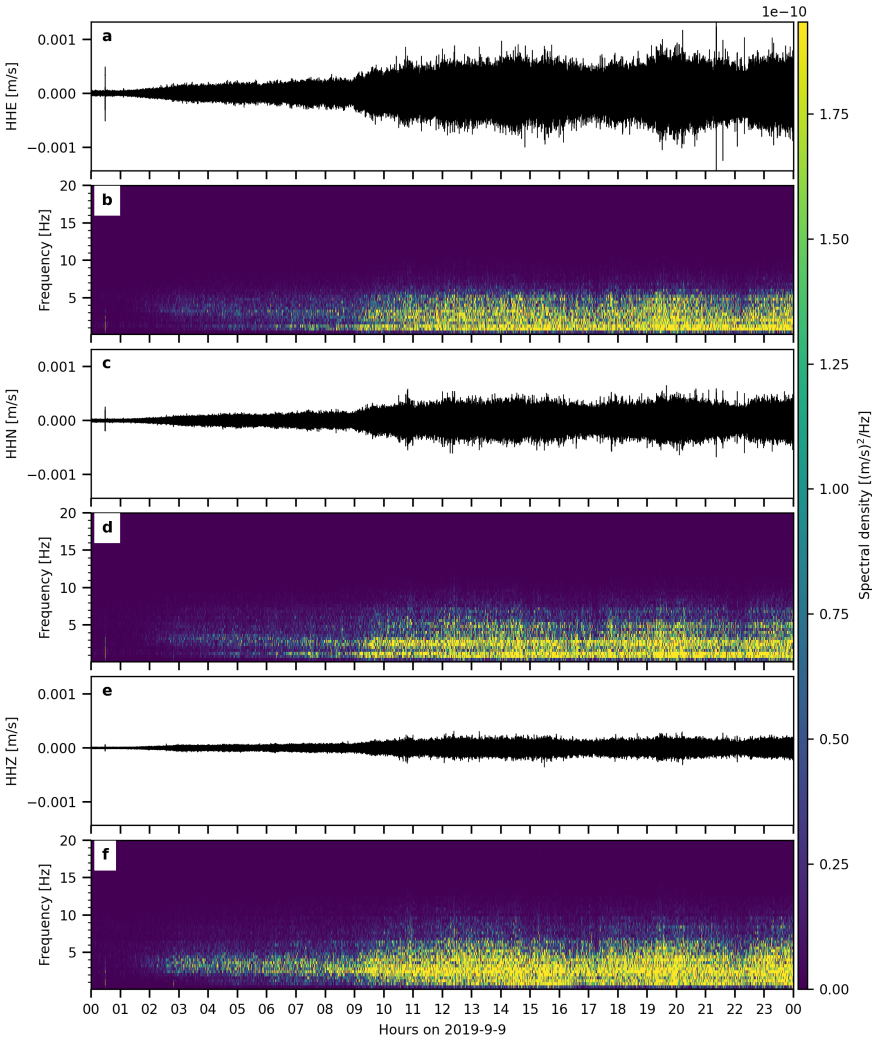

Figure S1: Seismograms and power spectrograms of the strong tremor on 2019-09-09 recorded at the Bb17 seismometer. Filtered from 0.1 to 20 Hz with a sliding window of 500 s and an overlap of 0.25.

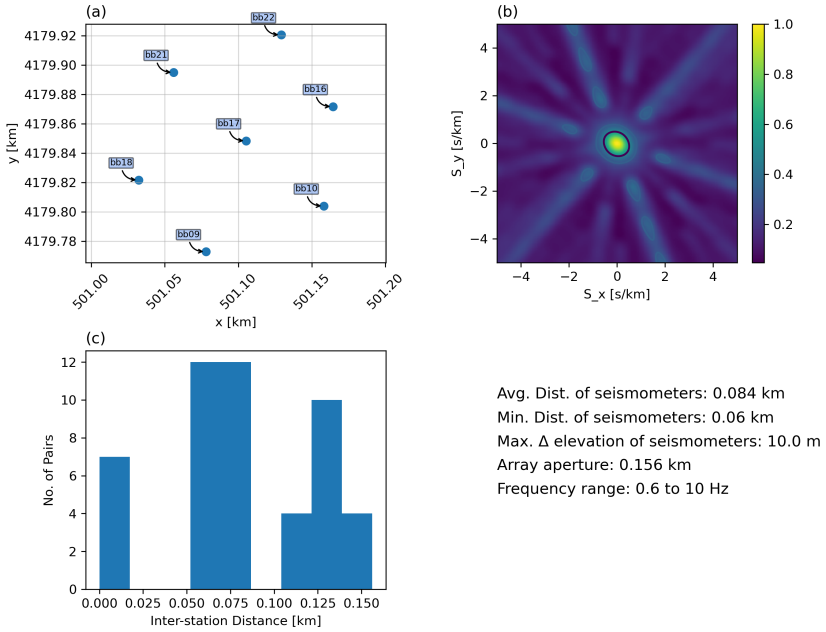

Figure S2: Array response for 0.6 to 10 Hz. (a) Array station set-up. (b) Array response on slowness grid with semblance indicated by colour. (c) Inter-station distance distribution.

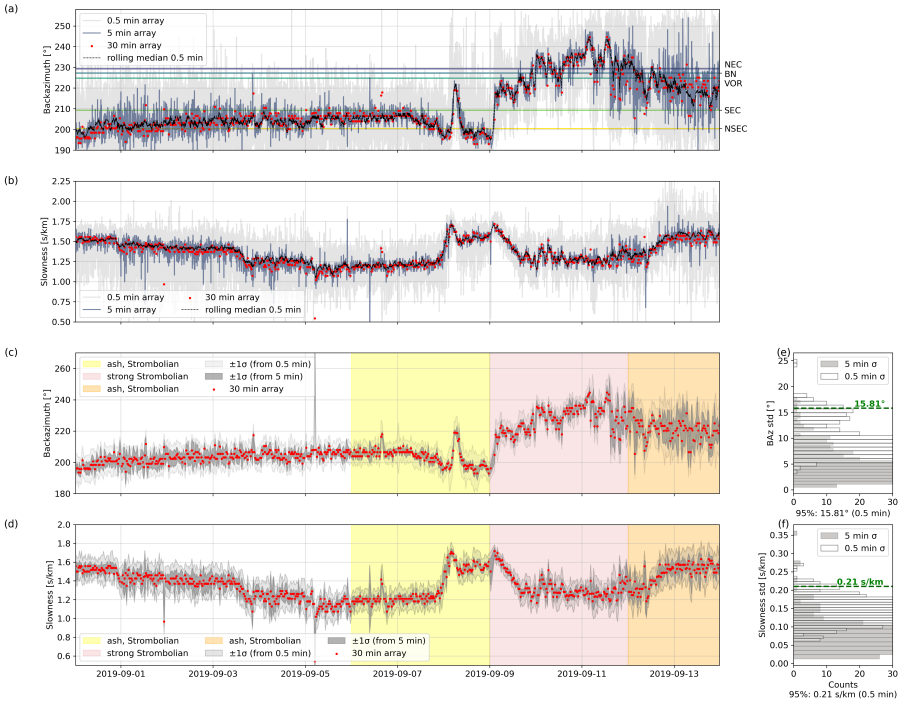

Figure S3: Comparison of BAz (a) and slowness (b) results from different sliding window times within the array analysis. (c,d) Standard deviation intervals for 0.5 and 5-min sliding time windows plotted for each 30-min sliding time window back azimuth (c) and slowness (d) result. Eruptive phases are shown as coloured blocks. (e,f) Histograms of the standard deviation for back azimuth and slowness.

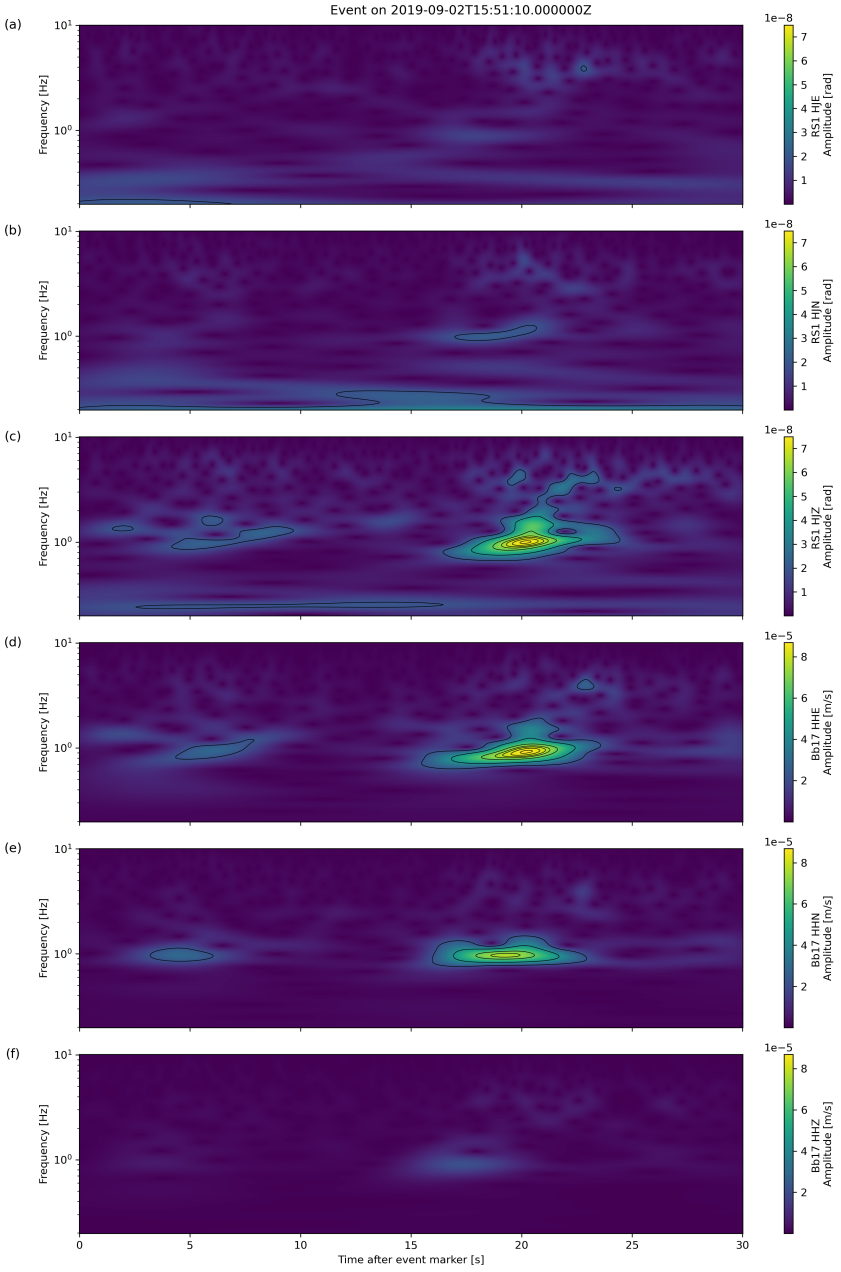

Figure S4: Morlet wave scalogram of the LP event on 2019-09-02 15:51 for the seismometer Bb17 and the co-located rotational sensor RS1 calculated from velocity-corrected and 0.2–10 Hz band-pass filtered data.

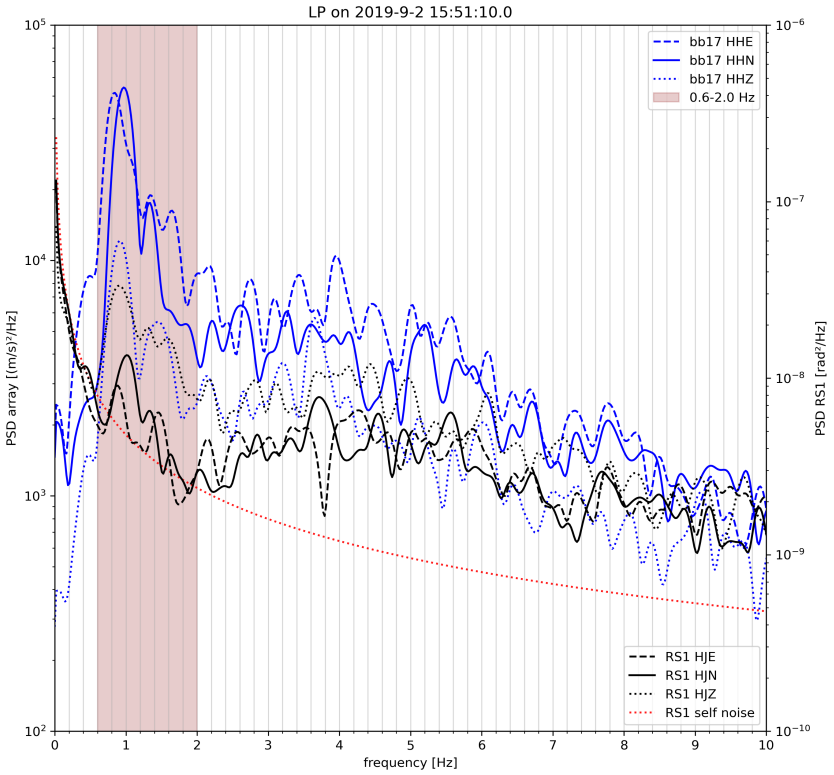

Figure S5: Comparison of power spectral densities (PSD) for all components of Bb17 seismometer and the rotational sensor RS1 for the LP event on 2019-09-02 at 15:51:10.

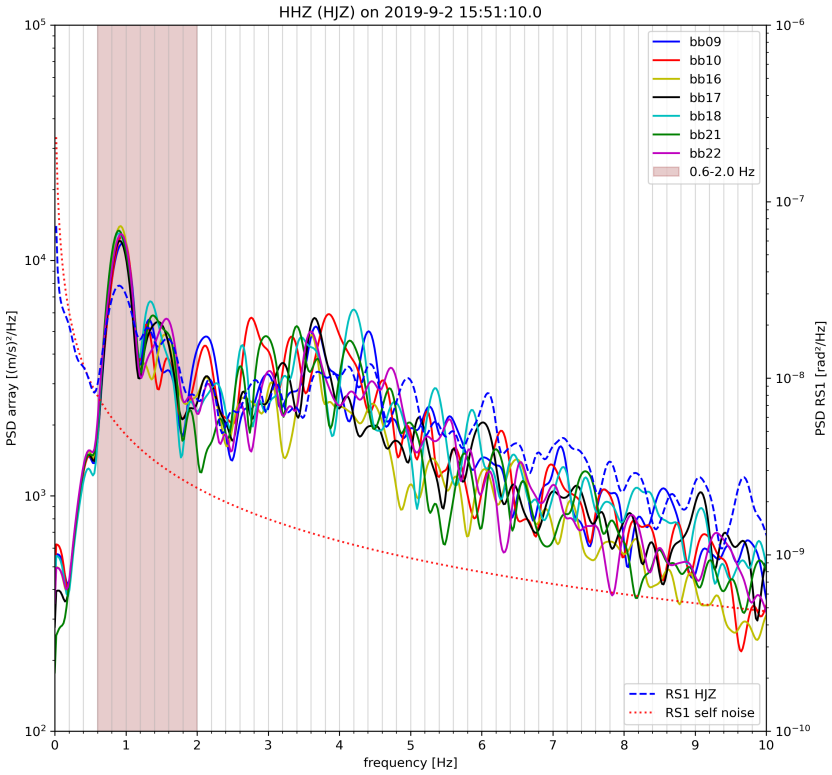

Figure S6: Comparison of power Spectral Densities for the HHZ component from all array seismometers and the rotational sensor component HJZ for the LP event on 2019-09-02 at 15:51:10.

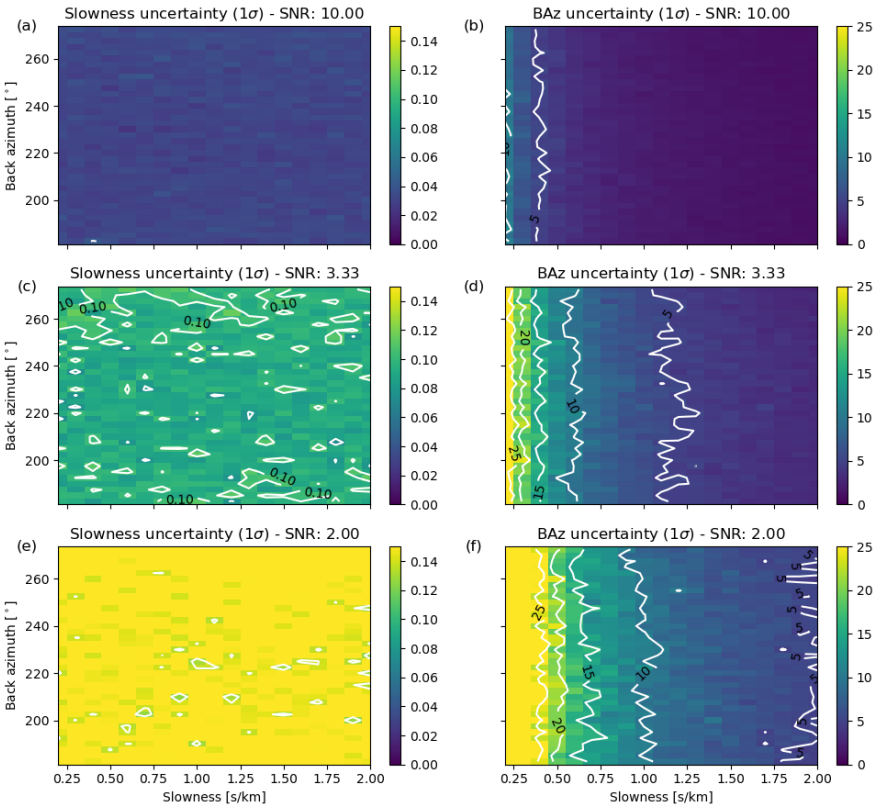

Figure S7: Slowness (a, c, e) and back azimuth (b, d, f) simulations for LP events with SNR 10 (a, b), 3.33 (c, d) and 2 (e, f). Contour lines represent slowness uncertainties above 0.1 s km^{-1} (a, c, e) and back azimuth uncertainties in 5° steps as indicated by numbers (b, d, f).

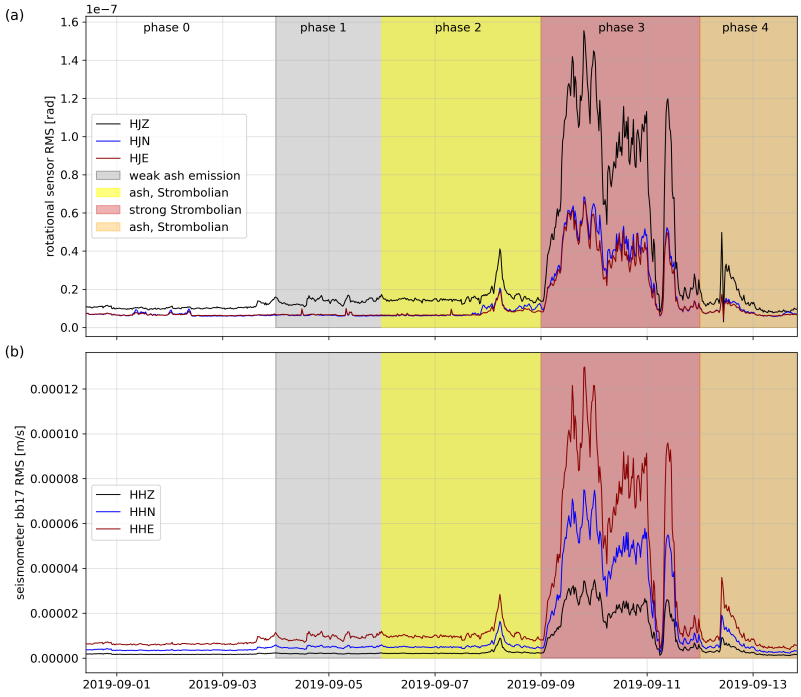

Figure S8: RMS for seismometer Bb17 and rotational sensor RS1 of the tremor signal, both filtered from 0.5 to 10 Hz.

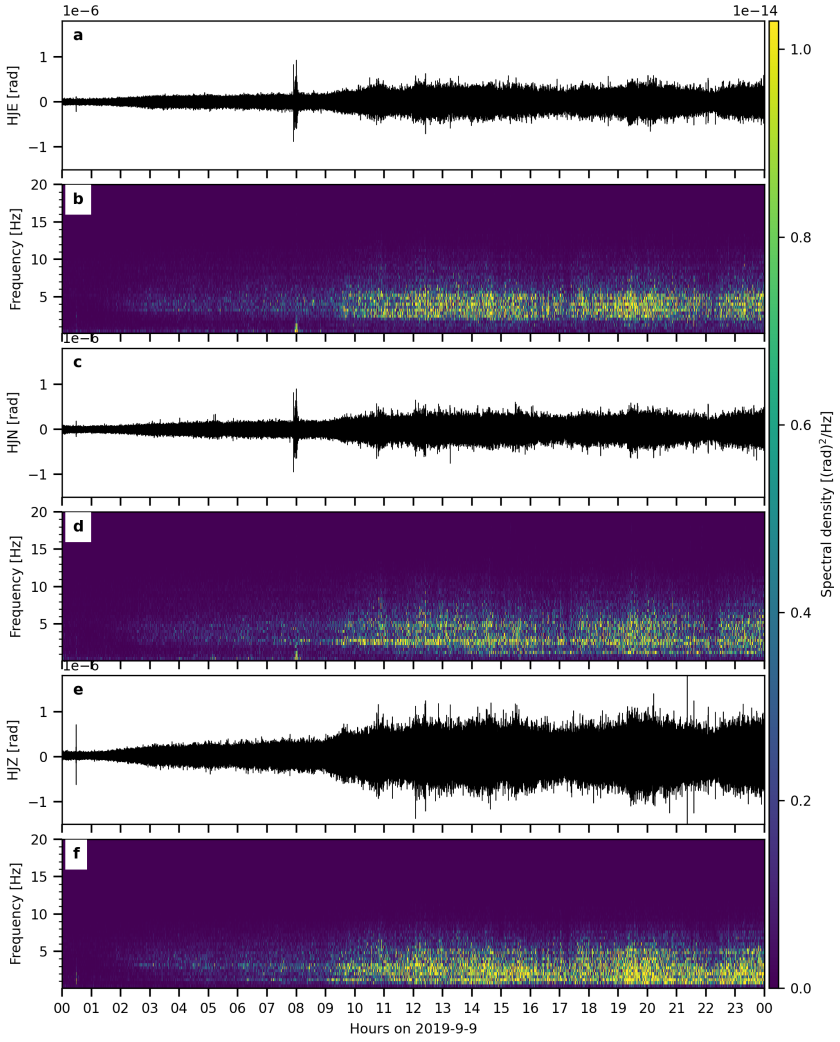

Figure S9: Seismograms and power spectrograms of the strong tremor on 2019-09-09 for the rotational sensor with the same settings as Fig. S1.

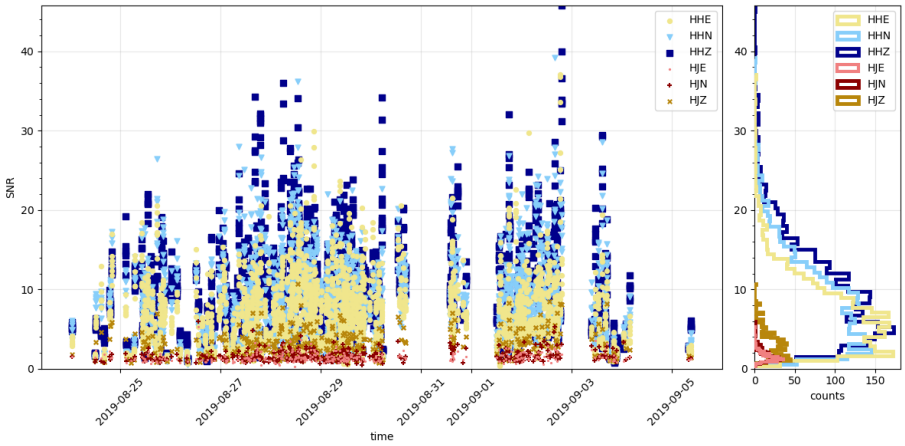

Figure S10: Signal-to-Noise Ratios for all LP events shown in colour according to array components and rotational sensor components.

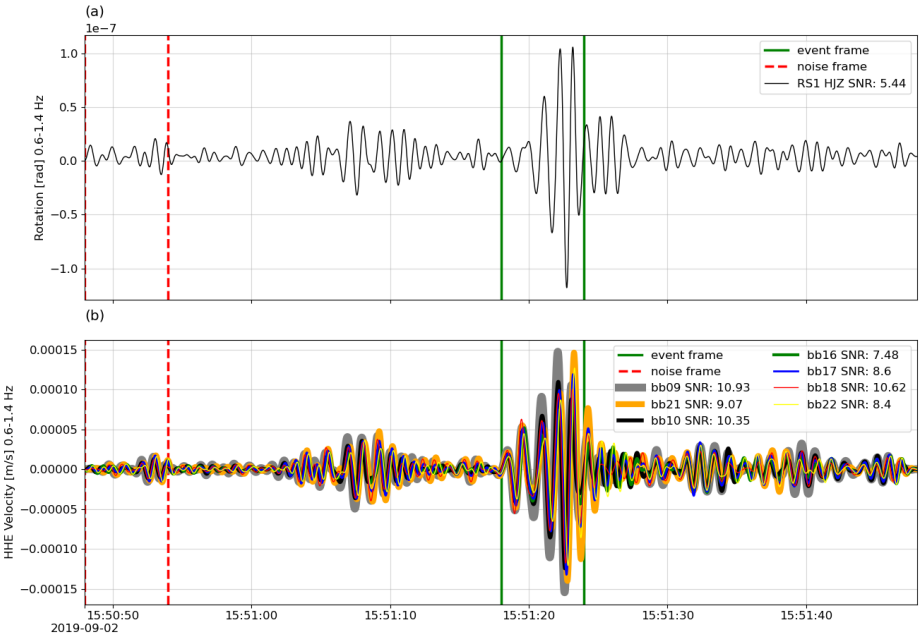

Figure S11: Waveforms of LP event on 2019-09-02 15:51 for the rotational sensor HJZ (a) and the seven HHE components of the array stations (b). Signal and noise time windows are marked by solid green and red dashed vertical lines, respectively.

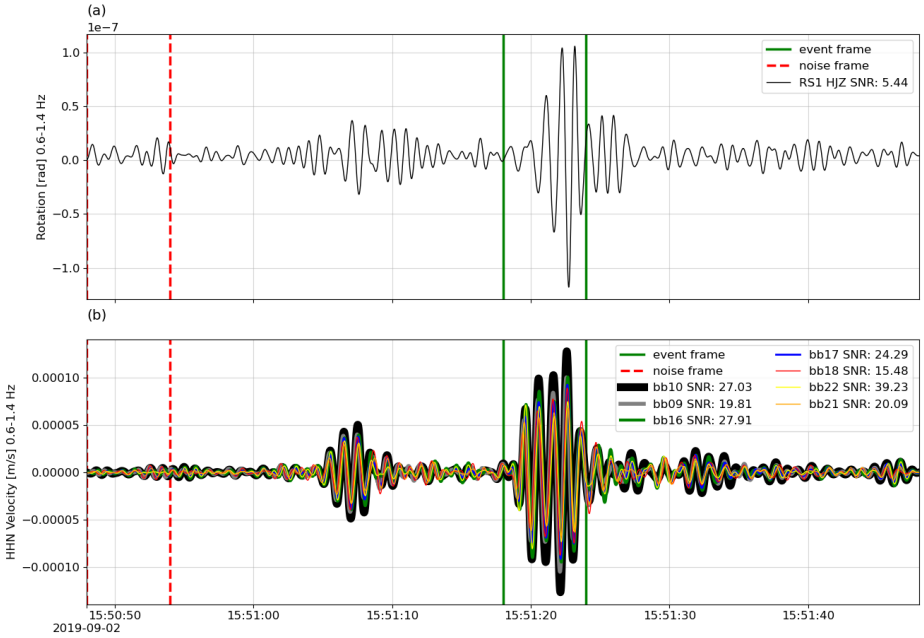

Figure S12: Waveforms of LP event on 2019-09-02 15:51 for the rotational sensor HJZ (a) and the seven HHN components of the array stations (b). Signal and noise time windows are marked by solid green and red dashed vertical lines, respectively.

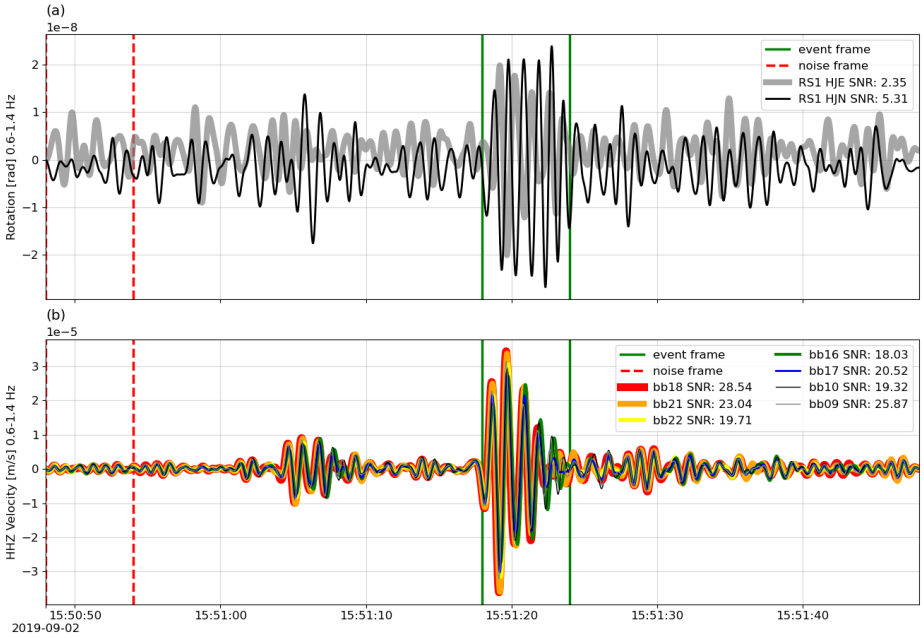

Figure S13: Waveforms of LP event on 2019-09-02 15:51 for the rotational sensor HJE and HJN and the seven HHZ components of the array stations. Signal and noise time windows are marked by solid green and red dashed vertical lines, respectively.

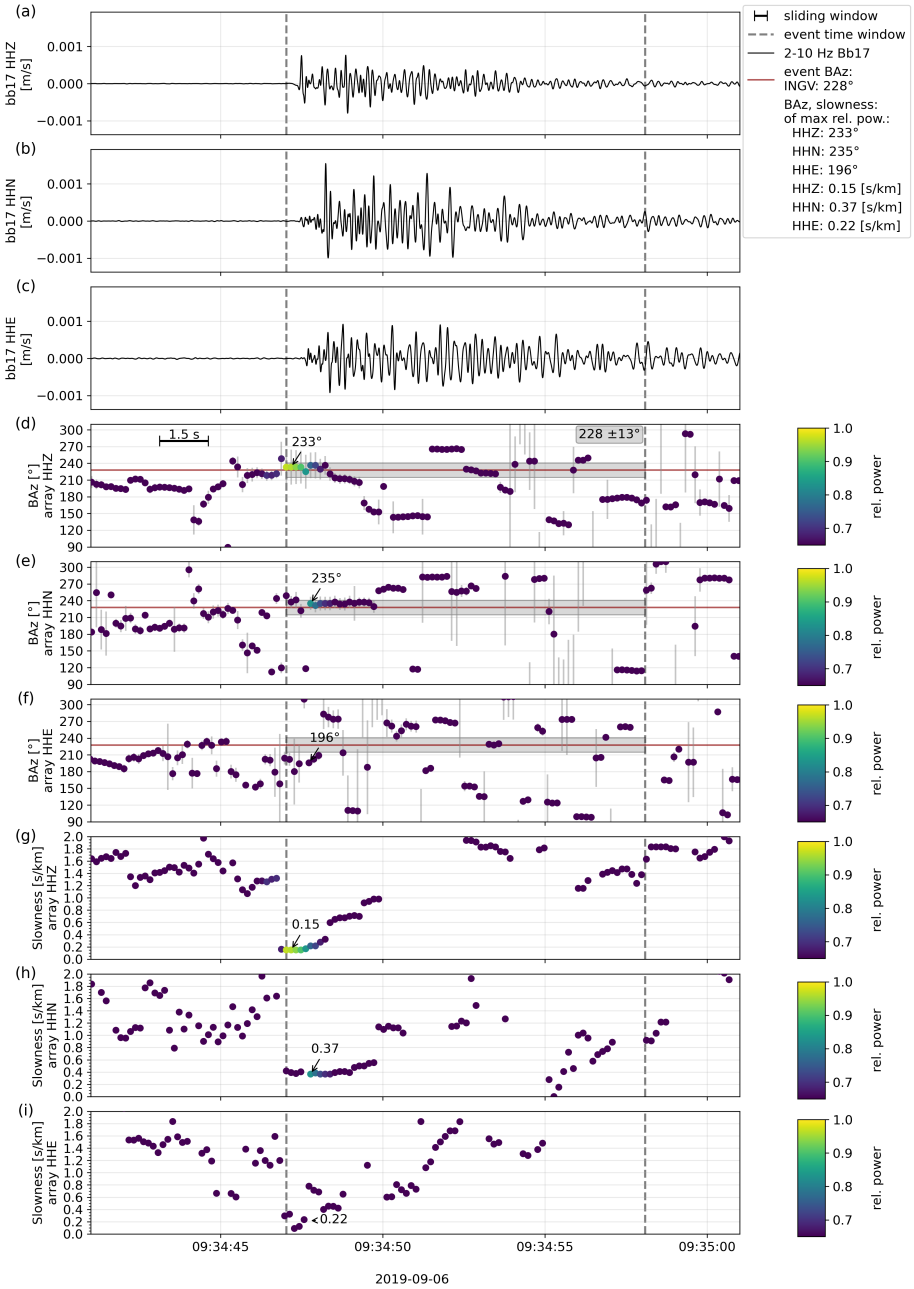

Figure S14: Exemplary VT event on 2019-09-06 09:34. Analysed by array processing for all three seismometer components. (a-c) Waveforms from station Bb17 filtered from 0.2 to 10 Hz. (d-f) Back azimuths obtained from array processing of all the components separately. (g-i) Slowness values from the processing for all three components. Colour indicates relative power.

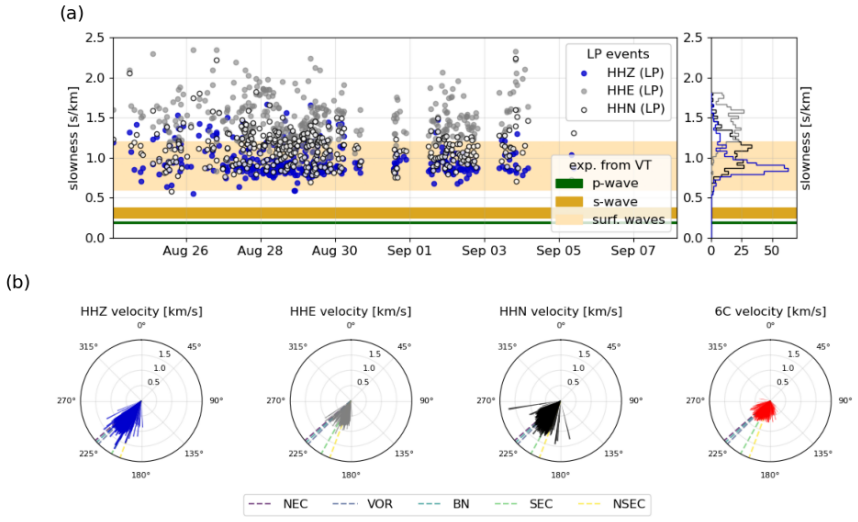

Figure S15: (a) LP event slownesses from the array beamforming of all components with expected wave type slowness ranges from the VT events in coloured plots. (b) Rose plots of directions from inverted slowness results of all array components and the 6C phase velocities.

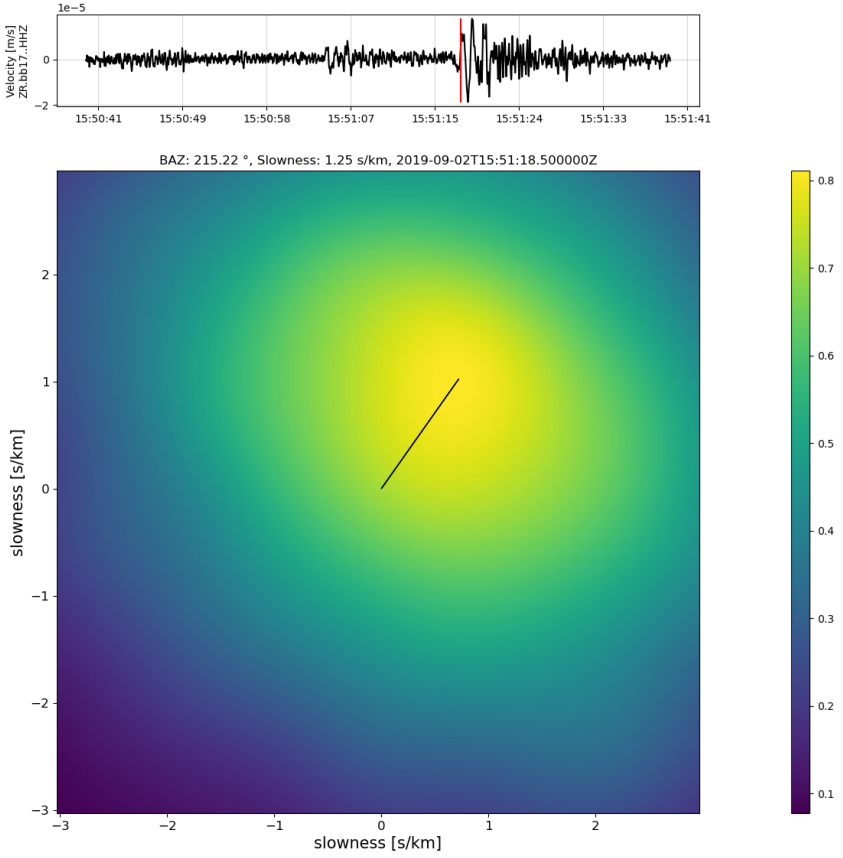

Figure S16: Array response for the LP event with 0.6 to 10 Hz on 2019-09-09 15:51:18.5.